Journal of Applied Polymer Science

# Formation of Continuous Dense Polymer Layer at the Surface of Hollow Fiber Using a Photografting Process

**Elsa Lasseuguette,[1,2] Jean-Christophe Rouch,[1,2] Jean-Christophe Remigy[1,2]**
[1]Université de Toulouse, INPT, UPS, Laboratoire de Génie Chimique, 118 Route de Narbonne, 31062, Toulouse, France
[2]CNRS, Laboratoire de Génie Chimique, 31030 Toulouse, France
Correspondence to: J.-C. Remigy (E-mail: remigy@chimie.ups-tlse.fr)

**ABSTRACT:** The surface modification of a PES hollow fiber by UV photografting has been investigated in order to graft a dense polymer layer. The study focused on a UV photografting process, starting from a monomer solution, enabling the thickness and regularity of the grafted polymer to be followed. 2-(Acryloyloxy)ethyl trimethylammonium chloride was polymerized on the surface of the PES membrane. Modified membranes were characterized by SEM, FTIR spectroscopy, and liquid and gas permeability. A dense layer of poly(2-(acryloyloxy)ethyl trimethylammonium chloride) was obtained when a photoinitiator and a photocrosslinker were used. Polymerization of the ammonium material also occurred inside the pores of the membrane. With pretreatment and an increase of the irradiation time, the thickness of the grafted polymer decreased and gas permeability reached measurable levels. However, a $CO_2/N_2$ selectivity of around 1 was found which suggested the presence of defects in the grafted layer. © 2014 Wiley Periodicals, Inc. J. Appl. Polym. Sci. **2015**, *132*, 41514.

**KEYWORDS:** fibers; grafting; membranes; photopolymerization; separation techniques

Received 23 May 2014; accepted 9 September 2014
**DOI: 10.1002/app.41514**

## INTRODUCTION

Atmospheric temperature increases during the last years have been associated with the growing levels of greenhouse gas emissions that can also be related to the worldwide demand for electricity. Unfortunately, this trend is expected to continue during the next decades and $CO_2$ is one of the main contributors to the greenhouse gases effect.[1] One way to reduce $CO_2$ emissions into the atmosphere is known as carbon capture and storage. Several approaches have been proposed to capture the $CO_2$ from fossil–fuel power plant emissions, including absorption, adsorption, cryogenic distillation, and membrane separation.[2] Nowadays, novel combinations of membrane and solvent absorption processes using a gas–liquid contactor have proved attractive and efficient.[3] Such technology is more flexible and compact and less energy consuming than alternative systems.

However, numerous limitations have been reported that might slow the processes occurring in gas–liquid contactors in industrial processes. The main issues are the wetting of the membrane, which increases the resistance to mass transfer, decreases process efficiency, and limits the long-term stability of the membrane. Two approaches are considered to solve the wetting problem: improving the resistance of the porous membrane or reducing the pore size by formation of a dense layer.[4,5] We focused our research on the densification of the membrane. The goal is to physically separate the gas and the liquid phases by a highly permeable dense membrane. To obtain high-performance membranes (high fluxes and productivity), the membrane should be very thin (i.e., in the micrometre range or below) so the mechanical resistance becomes dramatically low. In order to avoid this problem, a composite is used. The efficiency of this approach has been reported in several papers with a composite based on a polypropylene hollow fiber coated with TeflonAF©.[6–8] However, the dense layer is only coated on the outer surface of the hollow fiber and is bound to it with weak forces (Van der Waals links), which implies very low mechanical strength. For instance, if an inversion of pressure appears during the process of $CO_2$ capture, the coating can be blown off, destroying the contactor. One solution to this problem is to link the dense layer to the surface of the membrane with strong forces such as covalent bounds. For surface modification, photografting is a very successful technique. It presents several advantages: low cost of operation, mild reaction conditions, and permanent modification of the membrane surface chemistry. UV modifications have been used widely in membrane processes, for synthesis of pervaporation,[9,10] and reverse osmosis membranes,[11] for functionalization of ultrafiltration membranes for low fouling applications,[12] and for dye retention.[13] All grafted membranes from these references are obtained by a dip process although others methods have been used in the past.[14] Our project is

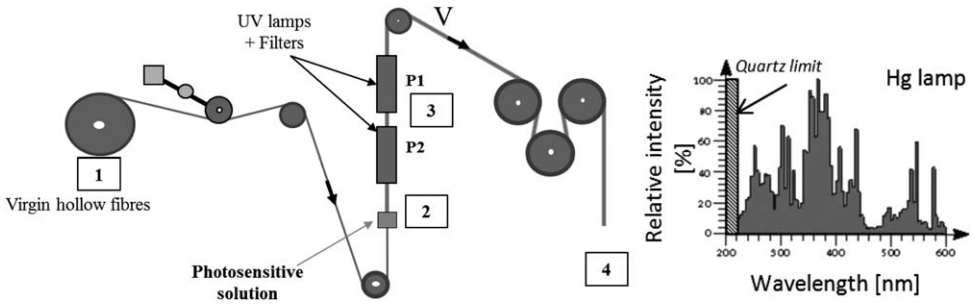


**Figure 1.** (Left) Grafting pilot. (Right) Relative intensity of the Hg lamp[19].

innovative in the way that we investigate the preparation of a composite with a dense layer using a continuous photografting process.

A composite based on a polyethersulfone support and a dense layer made of poly (2-(acryloyloxy)ethyl trimethylammonium chloride) was studied. Polyethersulfone (PES) presents good mechanical properties and is known to be easily functionalized by UV photografting.[14] 2-(Acryloyloxy)ethyl trimethylammonium chloride can be simply grafted by UV irradiation and the quaternary ammonium moieties have good $CO_2$ absorption performance.[15,16] Our laboratory has developed a new method for the continuous photografting process.[13] Surface modification was obtained by a vertical process with the fiber being drawn up through a liquid bath. The challenge of our project was to obtain a thin dense uniform layer without defects to be used in gas separation application or as a membrane contactor.

This paper deals with the process conditions required to obtain a continuous dense layer by a photografting method. Firstly, we describe the preparation of the composite, secondly the surface modification is analyzed by SEM microscopy and FTIR spectroscopy, and finally the separation performance (i.e., permeability and selectivity) of the composite is discussed.

## MATERIALS AND METHODS

### Materials

MicroPES® hollow fibers (PES) were purchased from Membrana. 2-(Acryloyloxy)ethyl trimethylammonium chloride (AETMA) (solution containing 20 wt % water), 4-hydroxybenzophenone (HB), *N,N*-methylene *bis* acrylamide (MBA), and methyl diethanolamine (MDEA) were supplied by Aldrich France and used as received.

### Photografting Process

**Photografting Process.** The continuous photografting of hollow fiber was carried out with a pilot described previously[13,17,18] (Figure 1).

First, hollow fiber (wetted or not) to be grafted (1) was passed through the photosensitive solution (2) at room temperature. A film of solution formed on the fiber surface as it was drawn out of the bath. The monomer present in film coat was photopolymerized and crosslinked by UV radiation with the passage of the fiber (3) through two polychromatic UV lights (Hg lamp model UVA Print LE, 5.5 kW, Hoenle UV France, Lyon, France). Quartz filters were used to block the UV irradiation below 220 nm.

The operating velocity was adjustable between 0.1 and 20 m $min^{-1}$, corresponding to an irradiation time ($T_{irr}$) in the range 600–3 s. Our system used an irradiation time of between 4 and 7.5 s; any longer and the fiber burned.

After grafting, the modified membrane was washed three times with reverse osmosis water in order to eliminate ungrafted homopolymer and unreacted materials.

**Photosensitive Solutions.** The solutions of the grafting materials (Figure 2) were prepared using 8 g of AETMA ($3 \times 10^{-2}$ mol) and 6.3 g of ultrapure water mixed with 0.17 g of Ret ($1.1 \times 10^{-3}$

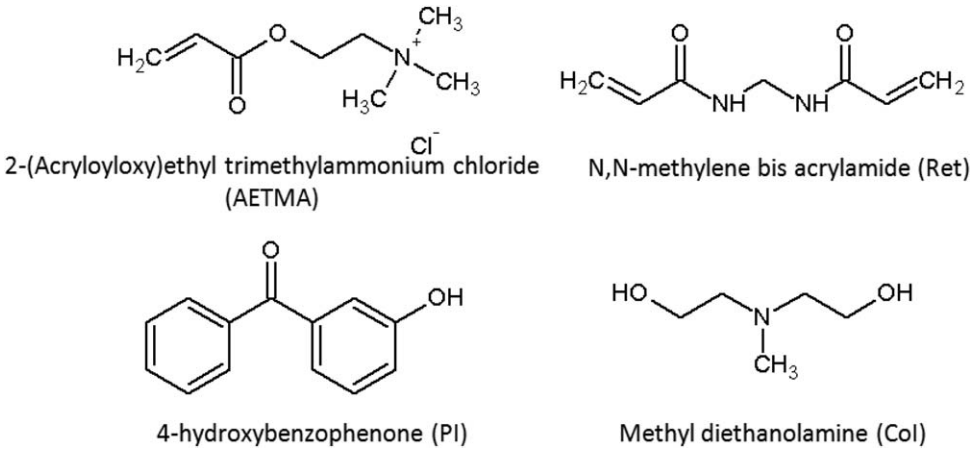


**Figure 2.** Chemical structures of the reactants.

**Table I.** Composition of Photosensitive Solutions

| N° | AETMA (concentration) | HB (concentration) | MBA (concentration) | MDEA (concentration) | Added water (mass) |
|---|---|---|---|---|---|
| 1 | 4 *M* | 0.06 *M* | 0.08 *M* | 0.12 *M* | 0 |
| 2 | 2.3 *M* | 0.06 *M* | 0 | 0.12 *M* | 6.3 g |
| 3 | 2.3 *M* | 0 | 0.08 *M* | 0 | 6.3 g |
| 4 | 2.3 *M* | 0.06 *M* | 0.08 *M* | 0.12 *M* | 6.3 g |

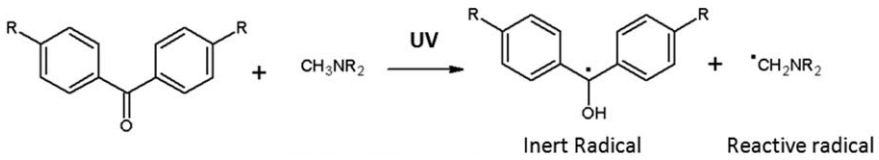


**Figure 3.** Type II initiator.

mol) at ambient temperature. After the dissolution of MBA, 0.18 g of HB ($9 \times 10^{-4}$ mol) was added then MDEA (0.22 g, $1.8 \times 10^{-3}$ mol) and the solution was mixed just before grafting.

The compositions of the solutions are reported in Table I.

4-hydroxybenzophenone was used as type II photoinitiator and a coinitiator, methyldiethanolamine, is used to generate a reactive radical by hydrogen abstraction (Figure 3).

**Photografting Mechanism.** The UV spectra of the polyethersulfone membrane and the photosensitive solution are reported in Figure 4.

The PES membrane, dissolved in dichloromethane, presents two absorption maxima at 227 nm and at 274 nm, which are due to the phenyl and the sulfonyl moieties respectively.[20,21]

Thanks to its photoreactivity, it is possible to modify the PES hollow fiber with UV. Yamagishi et al.[22] proposed a mechanism of photo-modification of poly(arylsulfone) with vinyl monomers (Figure 5). They explained that homolytic cleavage of a carbon–sulphur bond occurs with photoexcitation. This step yields two radical sites, one at the end of each polymer chain. Thus, both the aryl radical and the sulfonyl radical are reactive and can polymerize with the vinyl monomer.

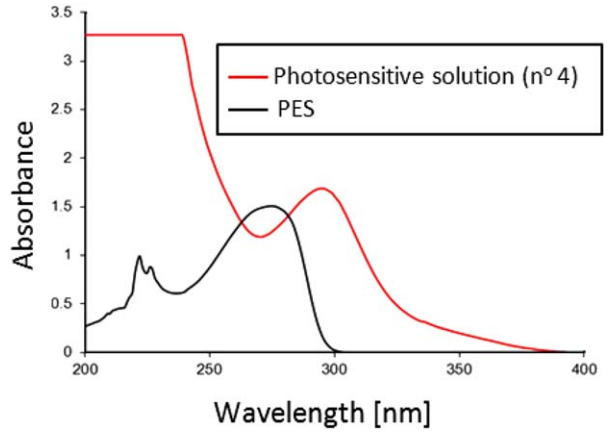


**Figure 4.** UV spectrum of PES hollow fiber (black) dissolved in spectroscopic dichloromethane and photosensitive solution (red) diluted in distilled water ([AETMA] = $9 \times 10^{-3}$ M]. [Color figure can be viewed in the online issue, which is available at wileyonlinelibrary.com.]

Comparison of the spectra (Figure 4) and the UV light emission of our pilot (Figure 1) shows that grafting between the PES membrane and the ammonium solutions can be successfully induced with our UV system.

Our goal was to obtain a dense layer of poly(2-(acryloyloxy)ethyl trimethylammonium chloride) ($PN^+$) at the membrane surface. For this purpose, a photoinitiator, hydroxybenzophenone, and a crosslinker, *N*,*N*-methylene *bis* acrylamide were used (Figure 6).

The photoinitiator was used to accelerate the UV grafting by initiating the ammonium monomer in solution. The crosslinker led to the formation of bonds linking the polymer chains thus helping to seal off any pores at the surface. According to the chemical reaction, we should obtain a dense layer ($PN^+$)

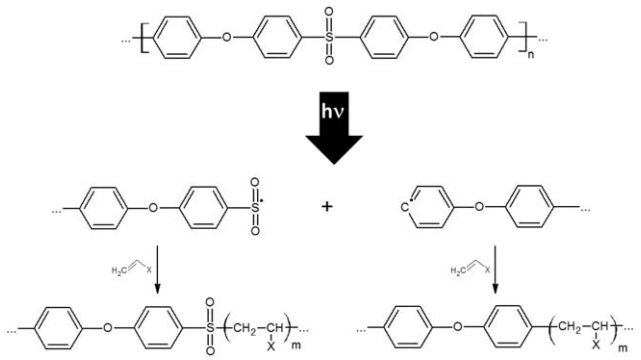


**Figure 5.** Mechanism of the UV photomodification of polyethersulfone.[21]

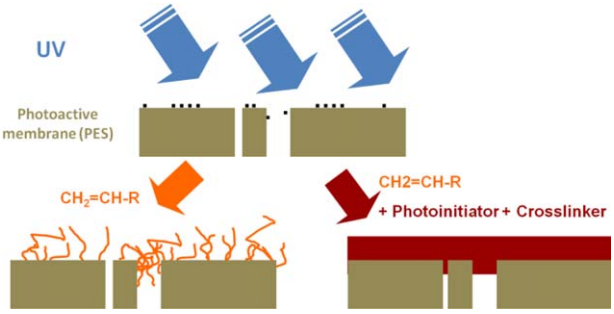


**Figure 6.** UV grafting of dense layer. [Color figure can be viewed in the online issue, which is available at wileyonlinelibrary.com.]

covalently bound to the PES with the following chemical structure (Figure 7):

The ammonium material appears ideal for $CO_2$ separation. Ghosal et al.[23] showed that the permeability to $CO_2$ is enhanced by the presence of amine moieties, presumably due to favourable interactions between acidic $CO_2$ molecules and basic $-NH_2$–R groups. Shishatskiy et al.[15] synthesized a polymer based on modified silica with a quaternary ammonium with selectivity to $CO_2$ over $N_2$ of 38. They explained the high selectivity by the fact that $CO_2$ is strongly sorbed on the active centres of the quaternary ammonium compounds.

### Analytical Techniques

**SEM Analysis and Depth of Grafting.** The surface appearance, thickness of the grafted fiber and the depth of grafting were examined using a scanning electron microscope (Hitachi TM1000). The fibers were first immersed in water, fractured in liquid nitrogen and then sputtered with a thin layer of gold.

The grafted layer was stained with iodine in order to differentiate it clearly from the starting fiber (Figure 8). The fractured fibers were dipped for 24 h in a 10% iodine solution then washed with distilled water until the pH was neutral. Iodine ions became chelated to the ammonium groups bound on to and within the membrane. The contrast between the grafted and the nongrafted part is then enhanced.

The grafted thickness was measured from the SEM image of a section. Two thicknesses were determined: $e_{dense}$, which corresponds to the thickness of the dense layer present at the surface of the fiber and $e_{depth}$, which is the thickness of the grafted part inside the fiber (Figure 9).

**Spectroscopic Analysis.** The surface was chemically analyzed by Fourier transform infrared spectroscopy combined with attenuated total reflectance (ATR) using a Thermo-Nicolet Nexus 670 spectrometer fitted with a DTGS detector and a diamond ATR crystal. The nominal incident angle was 45° and all spectra were recorded at 25°C. Forty scans between 3800 and 800 $cm^{-1}$ were obtained at a resolution of 2 $cm^{-1}$.

The UV spectra (spectrometer UV Light XTD5, Secoman, Seli) were obtained using distilled water and UV spectroscopic grade dichloromethane from Aldrich France.

**Liquid Permeability.** Water permeation was measured using PVC modules holding ten fibers 20 cm long. Water was fed into the outer side, and the operating pressure slowly increased in steps of 0.5 bar up to 2 bar. Each pressure was held for at least 2 min to check whether water had permeated through to the lumen side. The water permeability measurements were normalized at 20°C:[24]

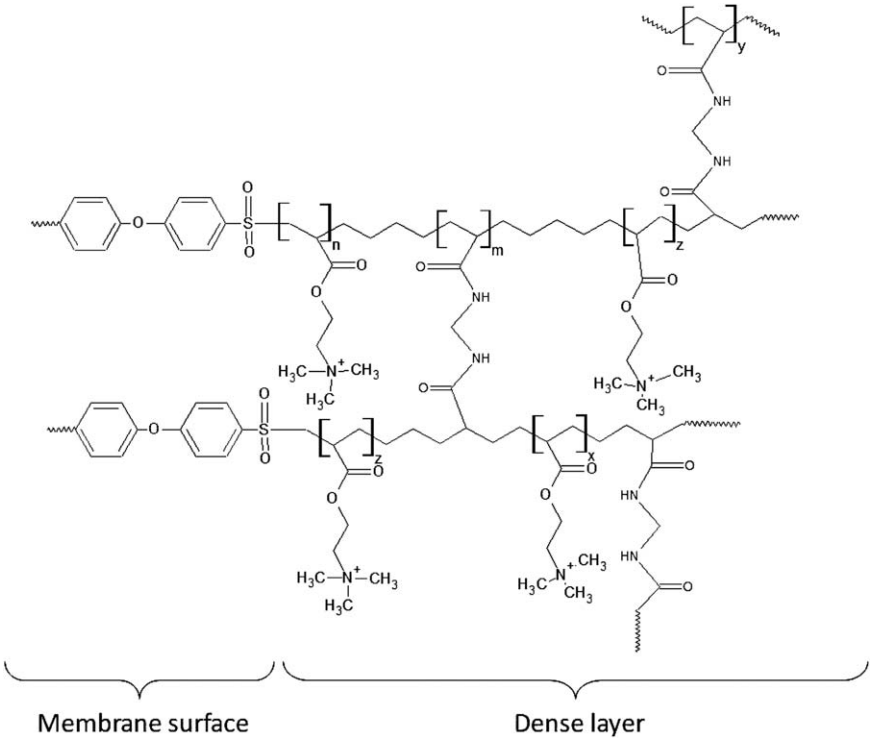


**Figure 7.** PN+ grafted membrane.

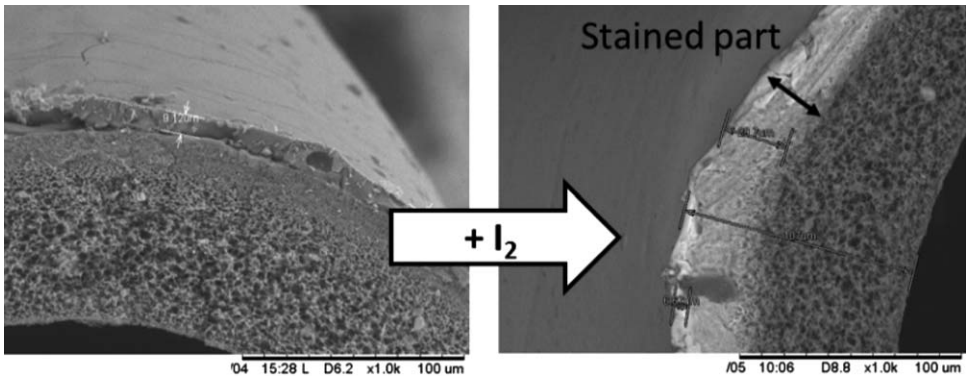


**Figure 8.** $I_2$ staining of the grafted layer.

$$J(20°C) = J(T)\exp(-0.0239(T-20)) \quad (1)$$

The lowest detectable water permeability was about 0.1 L $h^{-1}$ $bar^{-1}$ $m^{-2}$. Below this value the fiber was considered non-permeable towards liquid water.

**Gas Permeability.** The gas permeation of composite hollow fiber was measured using pure gases ($CO_2$, $N_2$). Laboratory-made stainless steel modules were used for the tests (Figure 10).

One or two 30-cm-long fibers were assembled in each module. The gas was fed into the shell side and the gas permeation flux was measured at the outlet of the lumen side. The pressure was increased slowly in 0.5 bar steps up to 10 bars. Each measurement was noted after 120 s of flux stabilization.

For a steady-state regime, the permeability (Perm($i$)) of component $i$ is calculated by equation (2):

$$\text{Perm}(i) = \frac{Q_{\text{perm}}}{S \times (P_{\text{feed}} - P_{\text{perm}})} = \frac{Q}{S \times P} \quad (2)$$

where $Q_{\text{perm}}$: flow rate of permeate [$NLh^{-1}$],

$P_{\text{feed}}$, $P_{\text{perm}}$: pressure of the feed and of the permeate, respectively [bar], $S$: exchange surface area [$m^2$].

Thus, the selectivity of the membrane for component $i$ relative to component $j$, $\alpha_{ij}$, is defined as the ratio of the permeability coefficient of these components by eq. (3):

$$\alpha_{i,j} = \frac{\text{Perm}(i)}{\text{Perm}(j)} \quad (3)$$

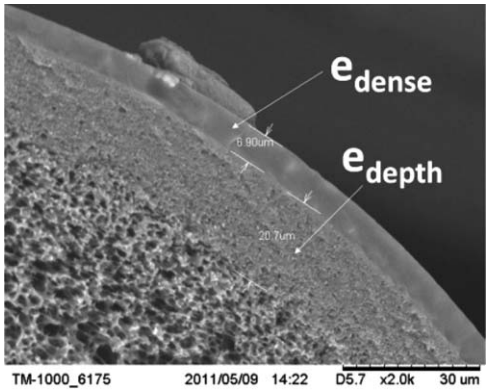


**Figure 9.** SEM image of cross section with $e_{\text{dense}}$ and $e_{\text{depth}}$.

## RESULTS

### Analysis of Dense Layer

The presence of the dense grafted layer (PN+) was confirmed by SEM analysis, ATR/FTIR analysis, and liquid permeability measurements.

**Surface and Thickness Analysis.** After each grafting, the modified membranes were characterized using SEM. The surface and section of the membranes were observed and the thicknesses measured from SEM images. The operating conditions are listed in Table II and representative SEM pictures shown in Figure 11.

Without the use of the photoinitiator (exp 1), very little grafted layer was formed and the fiber looked very similar to pristine fiber [Figure 11(b)]. This confirmed the fact that the photoinitiator is required for the activation of the monomer in the solution to induce the formation of the dense layer. In the same way, the absence of crosslinker (exp 2) led to absence of a dense layer [Figure 11(c)]. However, the liquid permeability of the modified membrane decreased compared to the pristine membrane. With $I_2$ staining, it was seen that the polymerization of PN+ occurred inside the pores of the membrane [Figure 11(c) $I_2$ staining].

For exp 3, droplets appeared along the fiber [Figure 11(e)]. Indeed, as the concentration of ammonium monomer was high, the solution became viscous. During the coating of the hollow fiber and when viscous forces are predominant, a hydrodynamic expulsion regime appears with liquid droplets being taken directly from the solution bath on to the fiber.[25,26] As the

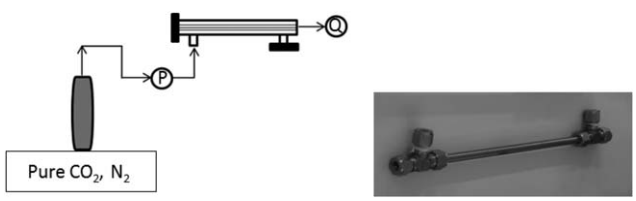


**Figure 10.** Setup for gas permeability experiments. [Color figure can be viewed in the online issue, which is available at wileyonlinelibrary.com.]

**Table II.** Operating Conditions for Grafting Process

| Exp n° | Solution (n°)[a] | $T_{irr}$ (s) | Pretreatment | $e_{dense}$ (μm) | $e_{depth}$ (μm) | Lp($H_2O$) (L $h^{-1}$ $bar^{-1}$ $m^{-2}$) (at 20°C) |
|---|---|---|---|---|---|---|
| 1 | 3 | 7.5 | - | 0 | 12 | 160 |
| 2 | 2 | 7.5 | - | 0 | 10 | 130 |
| 3 | 1 | 7.5 | - | Droplets | - | - |
| 4 | 4 | 7.5 | - | 7 | 25 | 0 |
| 5 | 4 | 6 | - | 5 | 20 | 0 |
| 6 | 4 | 5 | - | 4 | 20 | 0 |
| 7 | 4 | 4.3 | - | 0 | 0 | 2600 |
| 8 | 4 | 7.5 | Wetting | 3 | 10 | 0 |
| 9 | 4 | 6 | Wetting | 2 | 10 | 0 |

[a] See Table I for the composition, Lp($H_2O$) (MicroPES®) = 2250 L $h^{-1}$ $bar^{-1}$ $m^{-2}$.

droplets were stable with a cylindrical geometry due to surface forces, they kept their shape when polymerized.

In experiments 4–9 (except 7), a dense layer was obtained on the surface of the hollow fiber [Figure 11(d)]. The absence of defects in the dense layer was confirmed by the absence of measurable water permeability. With $I_2$ staining it was clear that UV irradiation penetrated the membrane. The pores of the membrane were filled with PN+ polymer (Figure 12). The figure shows that part of the membrane became white after $I_2$ staining. As explained above (see SEM analysis and depth of grafting), this coloration indicates the presence of PN+, which reacts with the iodine.

The UV irradiation reached 25 μm of depth. Yamagishi et al.[21] found that the irradiation of (2-hydroxyethyl methacrylate) under 254 nm for 10 min induced polymerization inside the PES membrane to a depth of 15 μm. It is interesting to note that for a dense PES polymer the UV only penetrated to 5 μm.[20] As shown in Figure 13, the depth of polymerization of PN+ increased with the irradiation time. Similarly, the dense surface layer was also seen to become thicker.

For exp 7, with a shorter time of irradiation, no dense layer was noted on $I_2$ staining. Thus, no polymerization occurred on the surface or in the membrane. The UV dose was too low to induce polymerization.

When the PES fibers were prewetted with water (exp 8 and 9), the depth of the modification in the membrane decreased. The presence of water in the pores hindered the absorption of the photoreactive solution by the membrane and slowed down polymerization inside the membrane.

**ATR/FTIR Analysis.** Infrared spectroscopy provided information about the chemical structure of the grafted membranes. ATR/FTIR spectra of the pristine PES hollow fiber, grafted PES, and AETMA are reported in Figure 14.

Figure 14 shows the appearance of new peaks ($v = 3300$ $cm^{-1}$, $v = 1720$ $cm^{-1}$, $v = 1660$ $cm^{-1}$, and $v = 950$ $cm^{-1}$) at the surface of the grafted membrane. The peaks at $v = 3300$ and $v = 950$ $cm^{-1}$ are due to the presence of ammonium moieties. The peak at 1720 $cm^{-1}$ is assigned to the ester linkage and the peak at 1650 $cm^{-1}$ to the amide bond. We also noted a decrease of the peak at 1620 $cm^{-1}$ which is assigned to the double bond of the monomer AETMA.

These modifications of the FTIR spectrum are coherent with the presence of the polymerized layer on the surface of the grafted PES hollow fiber.

For exp 7, the FTIR spectrum is similar to that of the pristine PES fiber. The peaks corresponding to the carbonyl moiety from the ester and the amide linkages are no longer present. Thus, as we saw before (paragraph 2.1.1), no polymerization occurred at the surface. The UV dose was too low to induce polymerization.

However, comparison between pristine and grafted PES showed that a new compound was present at the surface of the membrane. However, it was not possible to confirm that this compound was covalently linked to the PES fiber. Indeed, the grafting induced the cleavage of the sulfonyl moiety with the creation of a link between alkyl and sulfonyl groups (Figure 15). However, these two chemical bonds present similar IR absorption.

FTIR only confirmed the presence of a copolymer between AETMA and the crosslinker Ret at the surface of the PES membrane.

**Gas Permeability**

The pure-gas permeation ($CO_2$ and $N_2$) properties of composite hollow fibers are given in Table III in terms of permeability coefficients and selectivity over $N_2$.

The PES hollow fiber presented no selectivity. Indeed, as the mean diameter of the pores is equal to 0.2 μm [data from Membrana] the transfer is convective as the Knudsen number is higher than 1[24]. For exp 7, gas permeability did not change because, as we saw before, no polymerization occurred in or on the membrane.

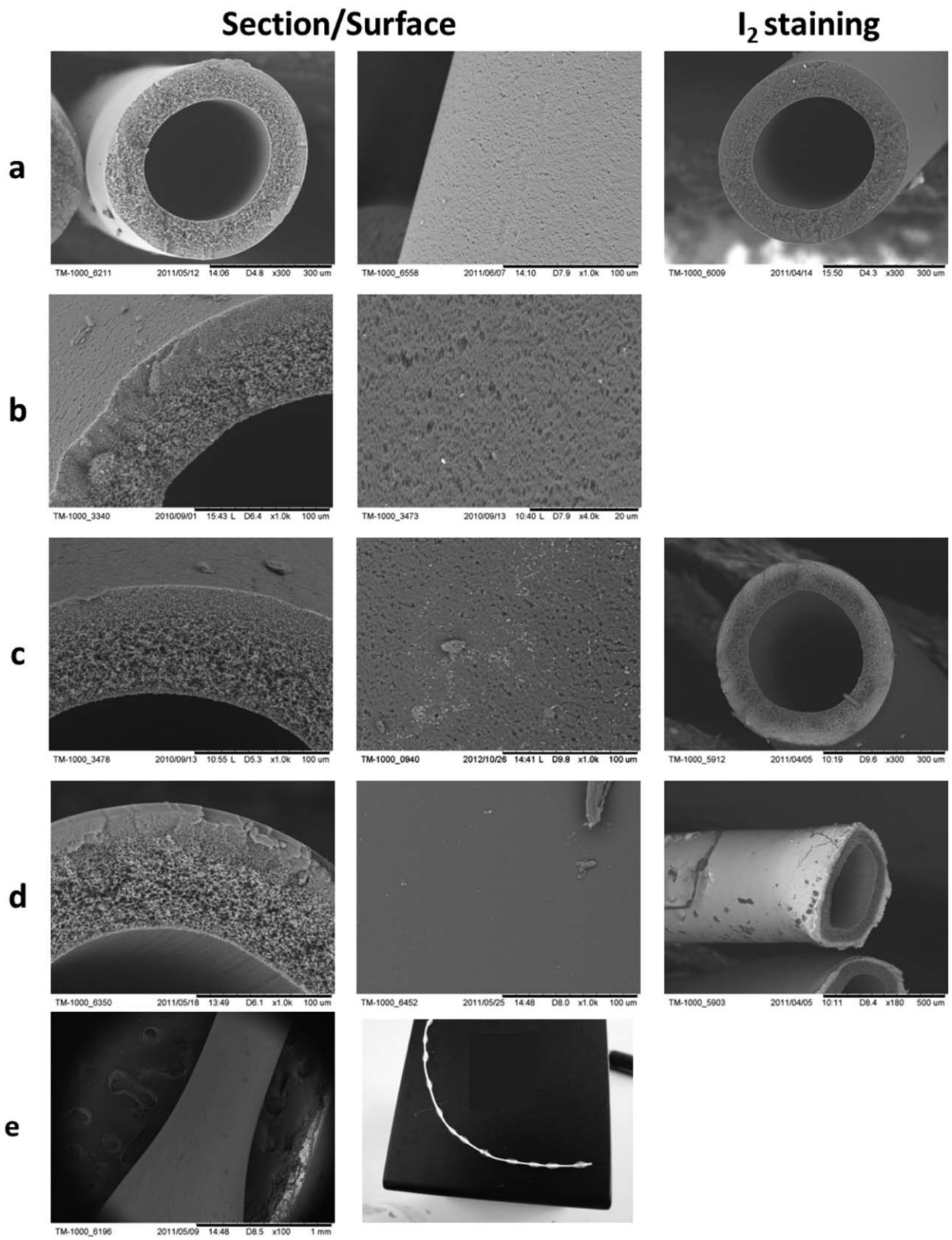


**Figure 11.** Scanning electron micrographs: (a) Pristine PES hollow fiber and (b–d) modified PES hollow fiber: *b* = exp 1, *c* = exp 2, *d* = exp 4–9, *e* = exp 3 (see Table II for the conditions of grafting).

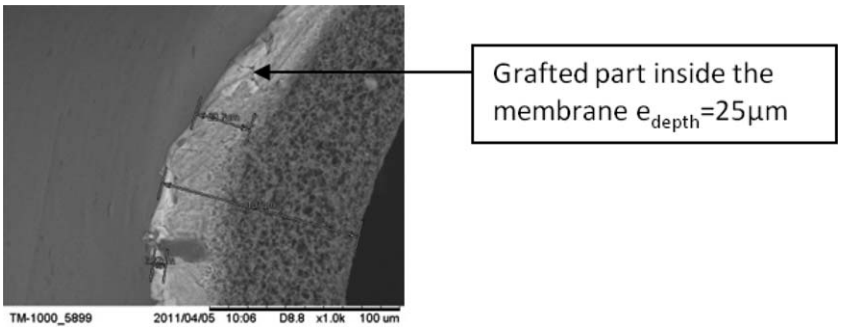


**Figure 12.** Stained membrane.

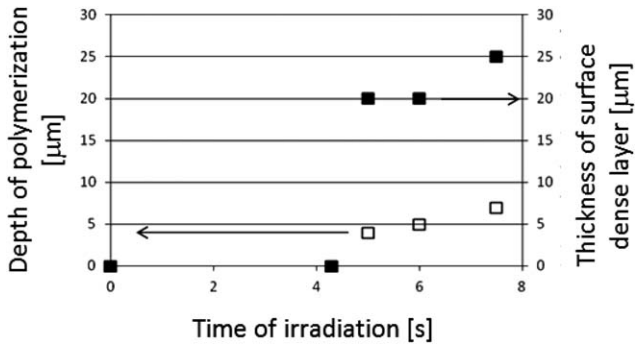


**Figure 13.** Depth of polymerization (solid squares) and thickness of the surface dense layer (empty squares) versus the irradiation time.

With grafting (exp 4, 5, and 9), there was a significant decrease in gas permeability, even reaching zero. In Figure 16, it can be seen that the increase of the polymerized material's thickness led to a decrease of the gas permeability. For exp 4 with the thickest polymerized materials, the presence of the dense coating induced high mass transfer resistance and no permeability was detected. This absence of permeability is due to the low sensitivity of our gas permeation pilot ($Q_{\text{mini detected}} = 0.5$ NL $h^{-1}$). Actually, if we plot gas permeability against the total thickness, the permeability of the modified hollow fiber 4 ($e_{\text{Total}} = 32$ $\mu$m) should be 31 NL $h^{-1}$ $bar^{-1}$ $m^{-2}$ for $N_2$ and 55 NL $h^{-1}$ $bar^{-1}$ $m^{-2}$ for $CO_2$. For our permeation experiments, these values correspond to a $N_2$ flow of around 0.6 NL $h^{-1}$ and a $CO_2$ flow around 0.4 NL $h^{-1}$.

One way to increase the gas permeability of the grafted membrane is to decrease the thickness of the dense layer. First, the velocity of the photografting was increased to decrease the time of irradiation (exp 5 and 7). Secondly, pretreatment by wetting pristine fibers with water was tested (exp 8 and 9) to prevent penetration of the monomer solution by capillarity thus reducing polymerization inside the membrane.

As seen before, exp 7 presented no dense layer because the irradiation time was too short. For exp 5, 6, 8, and 9, the thickness was decreased. The thinnest layer was achieved in exp 9 with pretreatment and a short irradiation time. A total grafted layer 12 $\mu$m thick was obtained. $CO_2$ and $N_2$ permeability (Table III) were 720 NL $h^{-1}$ $bar^{-1}$ $m^{-2}$ and 670 NL $h^{-1}$ $bar^{-1}$ $m^{-2}$ respectively.

However, as shown in Table III, the grafted membrane presented very little selectivity (compared to the ones previously obtained for quaternary ammonium salt which were of the order 38–56[15,16]), reaching a value of 1.1 for $CO_2/N_2$, i.e., the same as the pristine PES fiber. Selectivities of this order (1.1–1.5) indicate that defects such as large pores (pores with a diameter greater than the mean free path of the gas—of the order of 10–100 nm) are present in the polymerized layer.

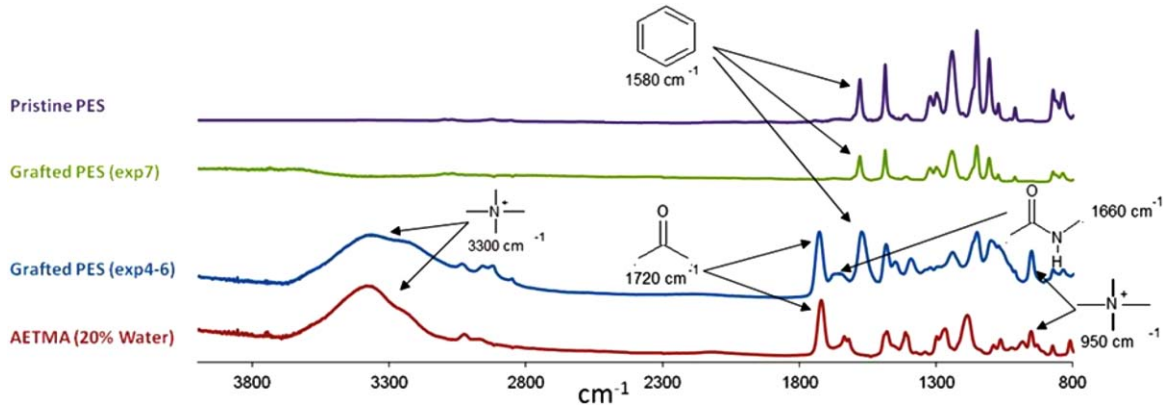


**Figure 14.** ATR/FTIR spectra of pristine PES hollow fiber, grafted PES hollow fiber (exp 4–7) and AETMA. [Color figure can be viewed in the online issue, which is available at wileyonlinelibrary.com.]

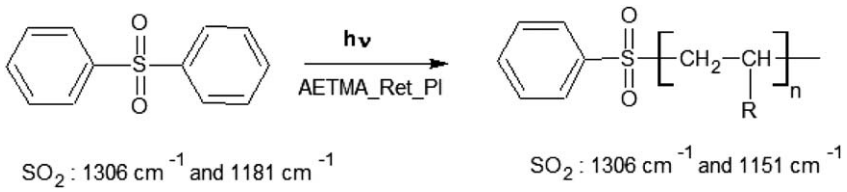


**Figure 15.** Cleavage of the sulfonyl moiety.

**Table III.** Gas Permeabilities and Selectivity of Pristine and Modified PES

| Exp | Total thickness[a] ($\mu$m) | Perm ($CO_2$) (NL $h^{-1}$ $bar^{-1}$ $m^{-2}$) Error = 16% | Perm ($N_2$) (NL $h^{-1}$ $bar^{-1}$ $m^{-2}$) Error = 26% | Selectivity $\alpha_{CO_2N_2}$ |
|---|---|---|---|---|
| Pristine PES | 0 | 77,000 | 84,000 | 0.9 |
| 4 | 32 | 0 | 0 | - |
| 5 | 25 | 450 | 290 | 1.5 |
| 7 | 0 | 75,000 | 83,000 | 0.9 |
| 9 | 12 | 720 | 670 | 1.1 |

[a] Total thickness is the sum of $e_{depth}$ and $e_{dense}$.

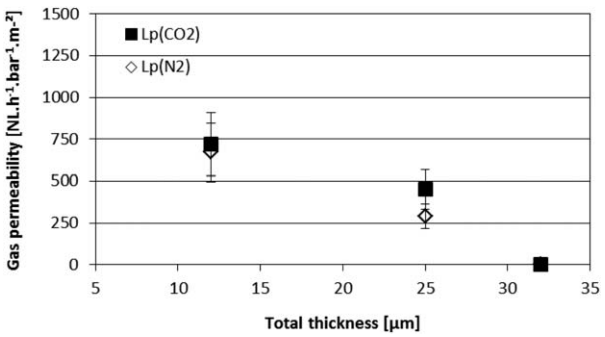


**Figure 16.** $N_2$ and $CO_2$ permeability versus total thickness.

## CONCLUSION

UV photomodification of polyethersulfone hollow fibers was performed in a continuous process with a semi-industrial pilot. The UV grafting consisted of the polymerization of 2-(acryloyloxy)ethyl trimethylammonium chloride with the use of a crosslinker and a photoinitiator. After the polymerization, a modified hollow fiber was obtained with a dense outer layer. The $I_2$ staining of the modified membranes showed that the polymerization also occurred within the membrane to a maximum depth of 25 $\mu$m. This depth was decreased to 10 $\mu$m with prewetting in water before grafting. FTIR analysis showed the presence of a copolymer based on the ammonium quaternary material with new peaks at 3300 and 950 $cm^{-1}$ related to the ammonium moieties, and 1720 and 1620 $cm^{-1}$ related to the ester linkage and the amide linkage, respectively. We showed that the presence of this polymer, and consequently the dense layer, required an irradiation time of over 4.3 s and the use of a photoinitiator and a crosslinking agent.

The dense layer led to a large decrease of the gas permeability until it was no longer measurable. To enhance gas permeability, thinner dense layers were obtained. However, no $CO_2$ selectivity was achieved due to the presence of defects. Another solution would be to increase the intrinsic permeability of the dense layer by adding plasticizers (Zeolites) or using a crosslinker with longer flexible chains (such as polyethylene glycol dimethacrylate). These materials could increase the microporosity of the dense layer, making it more permeable to gas.

## ACKNOWLEDGMENTS

The authors gratefully acknowledge financial support for this project by the ANR (Agence Nationale de la Recherche) through the AMELIE funding.

## REFERENCES

1. Davison, J. *Energy* **2007**, *32*, 1163.
2. Allam, R. J.; Bredesen, R.; Drioli, E. In Carbon Dioxide Recovery and Utilization, M. Aresta, Kluwer: Dordrecht, **2003**, p 55–118.
3. Ho, M. T.; Allinson, G. W.; Wiley, D. E. *Ind. Eng. Chem. Res.* **2008**, *47*, 1562.
4. Luis, P.; Van der Bruggen, B.; Van Gerven, T. *J. Chem. Technol. Biotechnol.* **2011**, *86*, 769.
5. Luis, P.; Van Gerven, T.; Van der Bruggen, B. *Prog. Energy Combust. Sci.* **2012**, *38*, 419.
6. Chabanon, E.; Roizard, D.; Favre, E. *Ind. Eng. Chem. Res.* **2011**, *50*, 8237.
7. Nguyen, P. T.; Lasseuguette, E.; Medina-Gonzalez, Y.; Remigy, J. C.; Roizard, D.; Favre, E. *J. Membr. Sci.* **2011**, *377*, 261.

8. Makhloufi, C.; Lasseuguette, E.; Remigy, J. C.; Belaissaoui, B.; Roizard, D.; Favre, E. *J. Membr. Sci.* **2014**, *455*, 236.
9. Yanagishita, H.; Kitamoto, D.; Ikegami, T.; Negishi, H.; Endo, A.; Haraya, K.; Nakane, T.; Hanai, N.; Arai, J.; Matsuda, H.; Idemoto, Y.; Koura, N. *J. Membr. Sci.* **2002**, *203*, 191.
10. Biao, Y.; Yang, W. *J. Membr. Sci.* **2003**, *218*, 247.
11. Setiawan, L.; Wang, R.; Li, K.; Fane, A. G. *J. Membr. Sci.* **2011**, *369*, 196.
12. Taniguchi, M.; Belfort, G. *J. Membr. Sci.* **2004**, *231*, 147.
13. Akbari, A.; Desclaux, S.; Rouch, J. C.; Remigy, J. C. *J. Membr. Sci.* **2007**, *297*, 243.
14. He, D.; Susanto, H.; Ulbricht, M. *Prog. Polym. Sci.* **2009**, *34*, 62.
15. Shishatskiy, S.; Pauls, J. R.; Pereira Nunes, S.; Peinemann, K. V. *J. Membr. Sci.* **2010**, *359*, 44.
16. Herrera-Alonso, J. M.; Sedlakova, Z.; Marand, E. *J. Membr. Sci.* **2010**, *349*, 251.
17. Goma Bilongo, T.; Remigy, J. C.; Clifton, M. J. *J. Membr. Sci.* **2010**, *364*, 304.
18. Béquet, S.; Remigy, J. C.; Rouch, J. C.; Espenan, J. M.; Clifton, M.; Aptel, P. *Desalination* **2002**, *144*, 9.
19. http://www.hoenle.de. Last accessed on March 2010.
20. Rivaton, A.; Gardette, J. L. *Polym. Degrad. Stab.* **1999**, *66*, 385.
21. Ulbricht, M.; Riedel, M.; Marx, U. *J. Membr. Sci.* **1996**, *120*, 239.
22. Yamagishi, H.; Crivello, J. V.; Belfort, G. *J. Membr. Sci.* **1995**, *105*, 237.
23. Ghosal, K.; Chern, R. T.; Freeman, B. D.; Daly, W. H.; Negulescu, I. I. *Macromolecules* **1996**, *29*, 4360.
24. Baker, R. W. Membrane Technology and Applications, 2nd ed.; Chichester: John Wiley and Sons, **2004**.
25. Lasseuguette, E.; Rouch, J. C.; Remigy, J. C. *Ind. Eng. Chem. Res.* **2013**, *52*, 13146.
26. Quéré, D. *Europhys. Lett.* **1990**, *13*, 721.